The Effects of Changing the Effective Crest Length of Labyrinth Side Weir on Discharge Capacity

Yusuf Dogan[1] · **Nihat Kaya**[2]

Abstract

Labyrinth side weirs have significant advantages according to conventional side weirs in terms of discharge capacity. Labyrinth side weirs are especially advantageous in places where more discharge is required from small weir openings lengths. The most significant feature of labyrinth side weirs is their effective crest length, which enables them to discharge more flow. In this study, the situation where the discharge capacity is decreased due to the narrowing of the crest length of the labyrinth side weir for any reason was experimentally investigated in detail. It was also considered that the potential narrowing could be in the upstream weir crest length. The overflow from the remaining length of the crest was enabled by the 1/3, 2/3, and 3/3 closure of the upstream crest length of the labyrinth side weir. Therefore, it was attempted to determine the decrease in discharge capacity due to the narrowing in the effective crest length. The values of the discharge coefficient were obtained by using the De Marchi approach. The study was conducted for subcritical flow regimes and steady-state flow conditions. A total of 980 experimental runs were conducted in this study. As the length of upstream effective crest length of the triangular labyrinth side weir at the straight channel decreases, the discharge coefficient also decreases. By narrowing the length of effective upstream crest length in 1/3, 2/3, and 3/3 ratios, the total discharge capacity decreased by approximately 10%, 23%, and 48%, respectively.

Keywords Labyrinth side weir · Crest length · Discharge coefficient · Discharge capacity

List of Symbols

b Width of a channel
C_d Side-weir discharge coefficient
F_1 Froude number at an upstream end of side weir
g Acceleration due to gravity
h Main channel depth
$h1$ Flow depth at an upstream end of side weir at channel center
$h2$ Flow depth at a downstream end of side weir at channel center
L Length (width) of side weir
ℓ' Triangular labyrinth side weir semi-crest length
p Height of weir crest

Q Discharge in the main channel
R Regression coefficient
S Decrease in discharge capacity (%)

✉ Yusuf Dogan
   ydogan@munzur.edu.tr

1   Department of Civil Engineering, Munzur University, Tunceli, Turkey

2   Department of Civil Engineering, Fırat University Elazığ, Elazığ, Turkey

1 Introduction

Weirs are among the oldest and simplest hydraulic structures that have been used for centuries [1]. Side weirs are used extensively in irrigation, land drainage, and sewage systems to provide the needed flow or to remove excess water in any channel [2, 3]. In addition, the excess flow caused by the superficial flow in the channels passing through the valley slopes is also removed through side weirs. It is possible to reduce these losses to the lowest level using side weirs to avoid water losses resulting from low-efficiency irrigation. There are various cross-sectional types of side weir. The hydraulic behaviors of different weir types also differ from each other. For this reason, the flow characteristic of a weir

type is important. This requires a separate examination of each weir, particularly the labyrinth side weir [2].

The form of the crest is one of the parameters affecting the flow discharge capacity. One of the ways to increase the discharge capacities of filled weirs is to increase the effective crest length of the weir [4]. For this purpose, weirs with various geometric plan forms are projected. Labyrinth weirs are the best way of doing this [5]. Coşar and Agaccioğlu [6] investigated the discharge coefficient of triangular weirs on straight and curved channels.

The ability of the labyrinth side weirs to discharge more flow in the same weir opening length depends on the effective crest length [7]. Thus, it is possible to close a certain section of the labyrinth side weir crest with bedding material if it has a mobile bedding material. Additionally, a part of the crest can stop working due to floating materials. The decreases in the crest length can result in decreases in discharge capacity. It is important to predict the side weir flow resulting from decreased crest length beforehand. Therefore, it is important to investigate experimentally the changes in the discharge capacities due to possible decreases in crest length.

In the last decade, numerous experimental and numerical studies were conducted on labyrinth side weirs. This subject has been an attractive field of study for researchers. Emiroglu et al. [8] studied the hydraulic characteristics of the triangular labyrinth side weir. The authors stated that decrease in the included angle of the labyrinth weir causes a considerable increase in discharge coefficient due to increasing the overflow length. Moreover, they reported that the discharge coefficient of the triangular labyrinth side weir is 1.5–4.5 times higher than conventional side weir. The labyrinth weir is a modern weir type and was first introduced by Emiroğlu et al.

$$
\begin{aligned}
C_d = \Bigg[& 18.6 - 23.535 \left(\frac{L}{b} \right)^{0.012} \\
& + 6.769 \left(\frac{L}{l} \right)^{0.112} - 0.502 \left(\frac{p}{h_1} \right)^{4.024} \\
& + 0.094 \sin\theta - 0.393 F_1^{2.155} \Bigg]^{-1.431}
\end{aligned} \tag{1}
$$

here the weir width (L), the channel width (b), the weir crest length (ℓ), and the height of the weir crest (p) are presented in meters while the included angle (θ) is in degrees and Froude number (F_1) is dimensionless.

Emiroglu et al. [9] discussed the discharge capacities of the one and two-cycle trapezoidal side weirs and the advantages of using one- and two-cycle labyrinth side weirs for the same weir opening length. They adopted the De Marchi approach [10] in the study they conducted and examined in detail whether one-cycle or two-cycle was more appropriate

in a given weir opening length. They obtained nonlinear reliable equations for both the single-cycle and the two-cycle trapezoidal labyrinth side weirs. The above-mentioned studies on the discharge capacities of the labyrinth side weirs were carried out for rigid base conditions. As a result of these experiments, they presented Eq. (2) for single-cycle labyrinth side weirs.

$$
\begin{aligned}
C_d = \Bigg[& -10.054 \left(Fr \frac{L_{ef}}{L} \right)^{0.039} - 0.001 \, Fr \left(\frac{L}{B} \right)^{-6.79} \\
& - 0.438 \left(\frac{L_{ef}}{L} \right)^{-0.284} + 0.52 Fr \left(\frac{y-p}{p} \right)^{-0.114} \\
& + 11.178 \left(Fr \frac{y-p}{p \sin\alpha} \right)^{0.013} \Bigg]^{-3.64}
\end{aligned} \tag{2}
$$

where Fr is the Froude number, L_{ef} is the effective length of the weir, L is the weir opening length, B is the channel width, y is the flow depth, p is the crest height of the side weir, α is the side weir included angle.

By utilizing Eq. 1 or 2, the discharge coefficient C_d can be calculated. Then, Q_w is calculated from the Poleni Equation. After that, by decreasing the value obtained for the ratio of 1/3 closed situation by 19%, Q_w can be calculated. Q_w can be calculated by a 32% for the ratio of 2/3 situation and a 42% decrease for the ratio of 3/3 situation. It should be considered that the triangle labyrinth side weir's total length should be used for L_{ef} in Eq. (3) (i.e., $L_{ef} = 2\,l$).

$$
Q_w = \frac{2}{3} C_d (y_1 - p)^{3/2} L_{ef} \tag{3}
$$

De Marchi is one of the earliest researchers who made theoretical studies to determine the discharge coefficient, assuming that the specific energy along the side weir remains constant. An approach was developed for the first time by De Marchi [10] for the closed solution of the water surface differential equation and Eq. (4) was obtained (De Marchi 1934) where C_d is the discharge coefficient, B is the main channel width, and L is the weir opening length. The equation for (Φ_i) is presented in Eq. (5).

$$
C_d = \frac{3}{2} \frac{B}{L} (\Phi_2 - \Phi_1) \tag{4}
$$

$$
\Phi_i = \frac{2E_i - 3p}{E_i - p} \sqrt{\frac{E_i - y_i}{y_i - p}} - 3 \sin^{-1}\left(\sqrt{\frac{E_i - y_i}{y_i - p}} \right) \tag{5}
$$

The present study aims (1) to investigate how the discharge capacity changes when the crest length of the labyrinth weir is narrowed at certain ratios. The study also aims (2) to examine the hydraulic characteristics of labyrinth triangular side weir for subcritical flow regime using the De Marchi approach, (3)
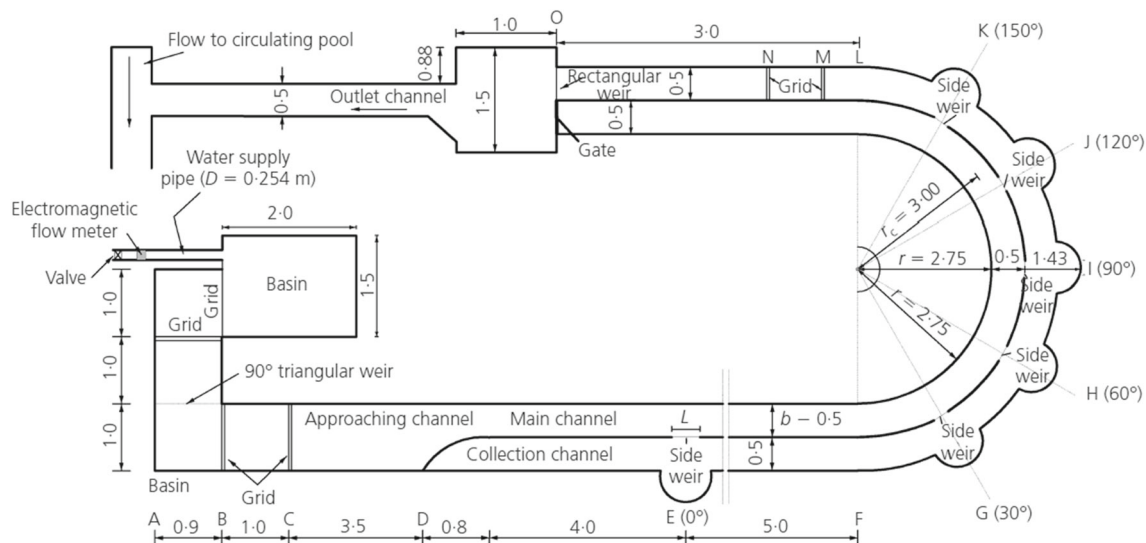
Fig. 1 Plan of the experimental setup (All dimensions are meters)

to determine the amount of reduction in discharge capacity for the weir crest length conditions to be tested. If the stream floor is a movable base; Swab materials from the main channel may accumulate in front of the weir crest, reducing the weir crest size. In this case, there can be no spillet along the entire crest. Similarly, a certain portion of the weir crest may be covered by debris. In this case, the effective weir length is reduced. In the current study, it is aimed to experimentally analyze how much the discharge capacity will decrease in such a situation. It was considered that the possible narrowing could be in the upstream crest length of the labyrinth side weir. Although certain studies [1 to 13] were conducted on side weirs in the literature, to the best of our knowledge, there has not been a study on the subject of the changes in the discharge flow in case of a narrowing in the crest length. In this study, the crest length of the labyrinth side weir was narrowed by the ratios of 1/3, 2/3, and 3/3. To shed light on this subject, 980 experimental runs were conducted.

2 The Experimental Setup and Procedure

This study was carried out in the Hydraulic Laboratory of Firat University using the experimental setup given in Fig. 1.

The length of this testing set was 18.20 m. The width of the main channel and collecting channel was 0.50 m and the slope of the channel was 0.001. The side walls of the main channel were covered with glass. The depth of the main channel was 0.50 m and the depth of the collecting channel was 0.70 m (see Fig. 1). The main channel and collection channel were separated by a thin sheet of metal. The tests were performed using a triangular labyrinth side weir. The triangular labyrinth side weir was positioned at a certain distance from the entrance of

the channel to provide fully developed flow conditions. The collecting channel that is on the opposite side of the parts where side weirs were placed was designed as a circle with a radius of 1.30 m (Fig. 1). The reason for this was to ensure a free nappe labyrinth side weir without any intervention to the flow. The flow depth was measured by a digital limnimeter (model Mitutoyo, accuracy of $\pm$ 0.01 mm) mounted on the measuring vehicle which can move in the x and y directions. The flow rate for the system was supplied from the pipe-tank pump system in the hydraulic laboratory. The main pipe diameter was 0.25 m. The discharge coefficient was measured with a Siemens electromagnetic flowmeter mounted on the feed line with an accuracy of $\pm$ 0.01 L/s.

The triangular labyrinth side weirs with various crest heights were placed on the separation wall. To provide steady-state flow conditions, perforated bricks were placed both in front of the upstream section of the channel and in the appropriate sections at the end of the collecting channel. The minimum nappe height was particularly taken as 0.03 m to minimize the surface tension effects which were not suitable for the prototype operations. Discharge coefficients in the tests ranged between 7 and 145 L/s and Froude numbers between 0.07 and 0.95. The tests were performed for triangular labyrinth side weirs with $L = 0.25, 0.50, 0.75$ m weir gaps, $p = 0.12, 0.16, 0.20$ m crest heights and $\alpha = 45°, 90°$ and 150° apical angles in the fixed base linear channel. The tests were carried out in the subcritical flow regime and steady-state flow conditions for free overfall conditions. The basin of the labyrinth side weir and main canal elevation was at the same levels. In the current study, the tests were performed for the states where the weir length was closed with three different sheet sizes and the weir length was not closed. In addition, the values of the specific energy at the upstream and

Table 1 Variable range studied

Variables	Values
Channel width, B (m)	0.50
Weir opening length L (m)	0.25, 0.50, 0.75
Labyrinth side weir's total weir crest length, ℓ (m)	0.3266, 0.6533, 0.9799
Weir height, p (m)	0.12, 0.16, 0.20
Slope of the channel base, J_o (—)	0.001
Main channel discharge coefficient, Q_1 (m^3/s)	0.007–0.145
Upstream Froude number, Fr (-)	0.07–0.95
Flow depth, y_1 (m)	0.15–0.28
Triangular labyrinth side weir included angle, $\alpha°$	45°, 90°, 150°

downstream were calculated and the relative specific energy value was significantly lower than 4%. Therefore, the De Marchi approach was used with confidence (Table 1).

First, the crest lengths were closed in three steps (1/3, 2/3, 3/3) for side weirs with three different crest heights. The depth readings were made at the axis and inner bank. The fully open state of the crest length was shown as LW Type 1. The state of closing the upstream crest length by the ratios of 1/3, 2/3, and 3/3 were named LW Type 2, LW Type 3, and LW Type 4, respectively. As shown in Fig. 2, the upstream crest length was closed with plates. The plates were made of 3 mm thick steel material and painted to prevent corrosion. The graphs were drawn and comparisons were made using the data obtained from the tests performed by Emiroglu et al. [11] on the fully open status of the crest length ($p = 0.12$, 0.16 and 0.20 m).

As can be seen in Fig. 3, water depth measurements were conducted on the points at the sides of A1-A3, B1-B3 and C1-C3 side weirs through the A2, B2 and C2 canal central lines by using limnimeter. Limnimeter readings were obtained by utilizing a special mechanism that can move bilaterally on the rail.

The tests were carried out in the subcritical flow regimen and steady flow conditions for the state of free overfall. Novak and Cabelka [12] have shown that the minimum nappe height should not be less than 0.03 m. For this reason, the minimum nappe height was taken as 30 mm. After a good physical description of the labyrinth side weir flow in the linear rectangular channel, a series of tests were performed to obtain the labyrinth side weir discharge coefficients, different Froude numbers, different p/y_1 ratios, and the discharge coefficient variation of different ℓ/L ratios cfvc.

3 Results and Discussion

In this study, the experiments were carried out in order to study the effect of upstream crest lengths on discharge coefficient in the triangular labyrinth side weirs, particularly considering the Froude number (Fr), non-dimensional crest height p/y_1, non-dimensional weir length (L/B), non-dimensional effective crest length of triangular labyrinth weir ($2\ell'/L$), and included angle (α).

Increasing the effective crest length causes an increase in discharge capacity. As the included angle decreases, the crest length increases. Therefore, discharge capacity values at small included angles are higher than at large angles. Similarly, any contraction in the crest causes a decrease in the discharge capacity.

The comparison of the completely open situations and the ratios of 1/3, 2/3, and 3/3 closed situations by utilizing the Fr-C_d graphs can be seen in Fig. 4a–c. To calculate the percentage of decrease due to crest narrowing, all of these graphs were drawn and only 3 of the graphs were presented to provide examples. As can be seen in Fig. 4a–c, with the decrease in the crest length of the labyrinth side weir, decreases in flow coefficient values were observed. It was concluded that the narrowing rates of crest length and decreased rates in discharge capacity were coherent.

By utilizing the graph drawn in Fig. 4a–c, by considering the completely open situation and 1/3, 2/3, and 3/3 closed situations, respectively, the mean rates of decreases in discharge capacity were calculated. These calculations were first conducted for each experimental series. Then, the rate of decrease in the rate of closure was calculated in percentages. The decreases in discharge capacity are calculated according to Eq. 2.

$$S = \frac{C_{d2} - C_{d1}}{C_{d2}} \times 100 \tag{6}$$

S = Decrease in discharge capacity (%).

The values calculated are presented in Table 2. When the data were examined, it was discovered that the decrease rates were 19%, 32%, and 42% for 1/3, 2/3, and 3/3 closure of effective crest length, respectively. These ratios were obtained by calculating the arithmetic means of decrease ratios in percentage, which were calculated for each closure situation.

Fig. 2 Variation of the crest lengths in triangular labyrinth side weirs
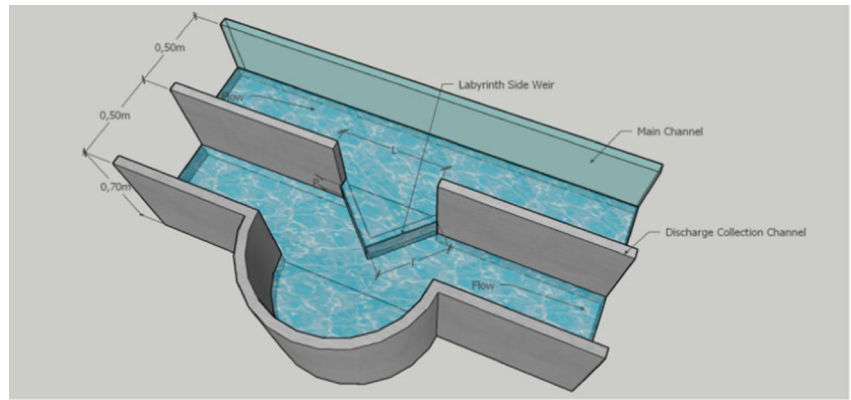
(a) LW Type 1
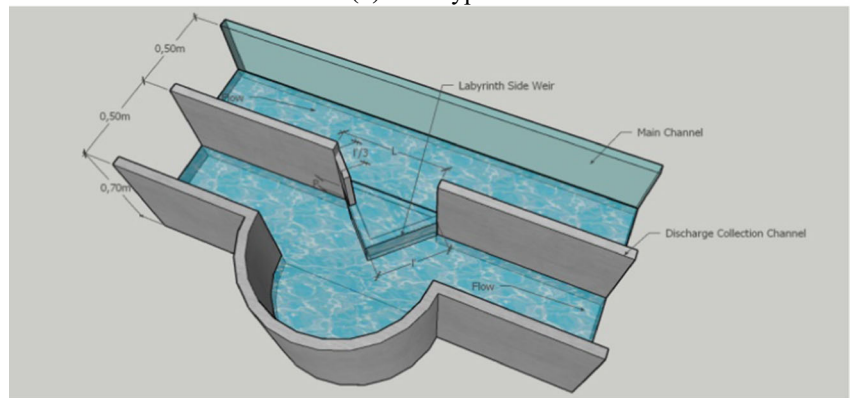
(b) LW Type 2

(c) LW Type 3

(d) LW Type 4

Fig. 3 Places where depths are measured

Fig. 4 **a–c** Comparison of LW Type 1 and LW Type 2, 3 and 4

Table 2 Data for the calculation of means according to closure situations

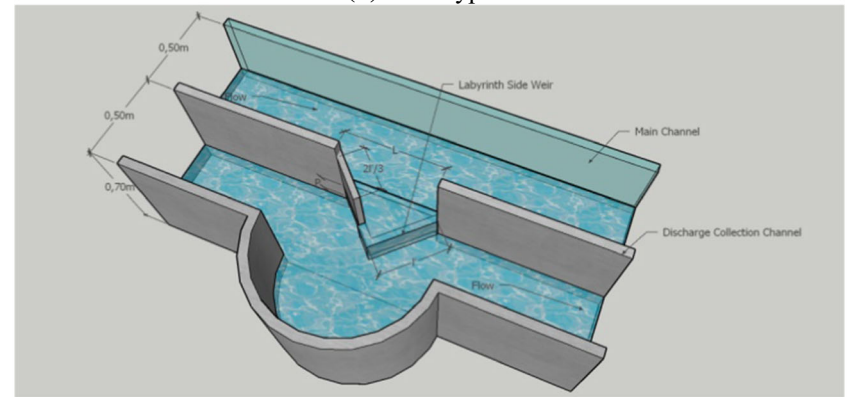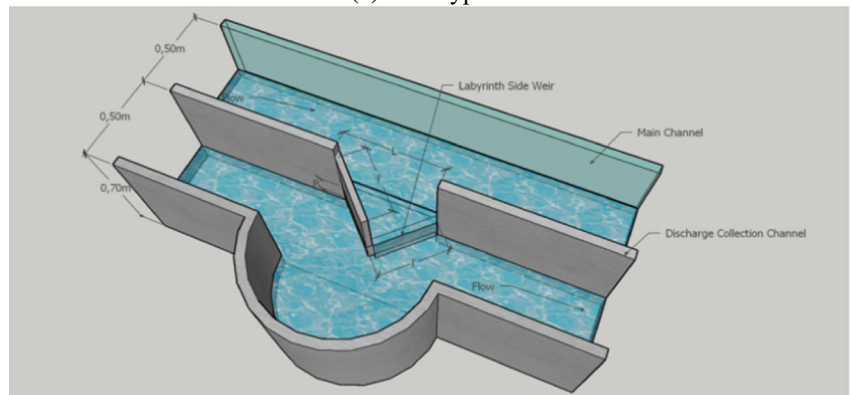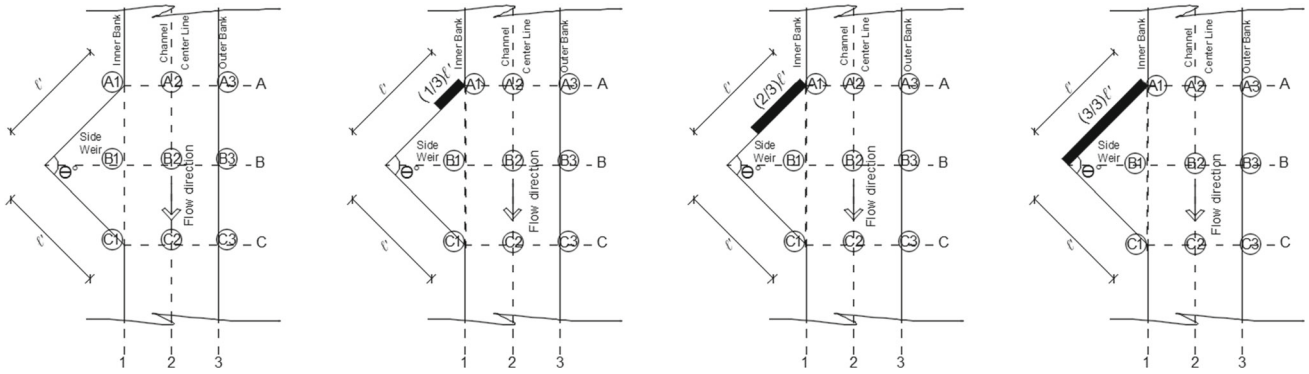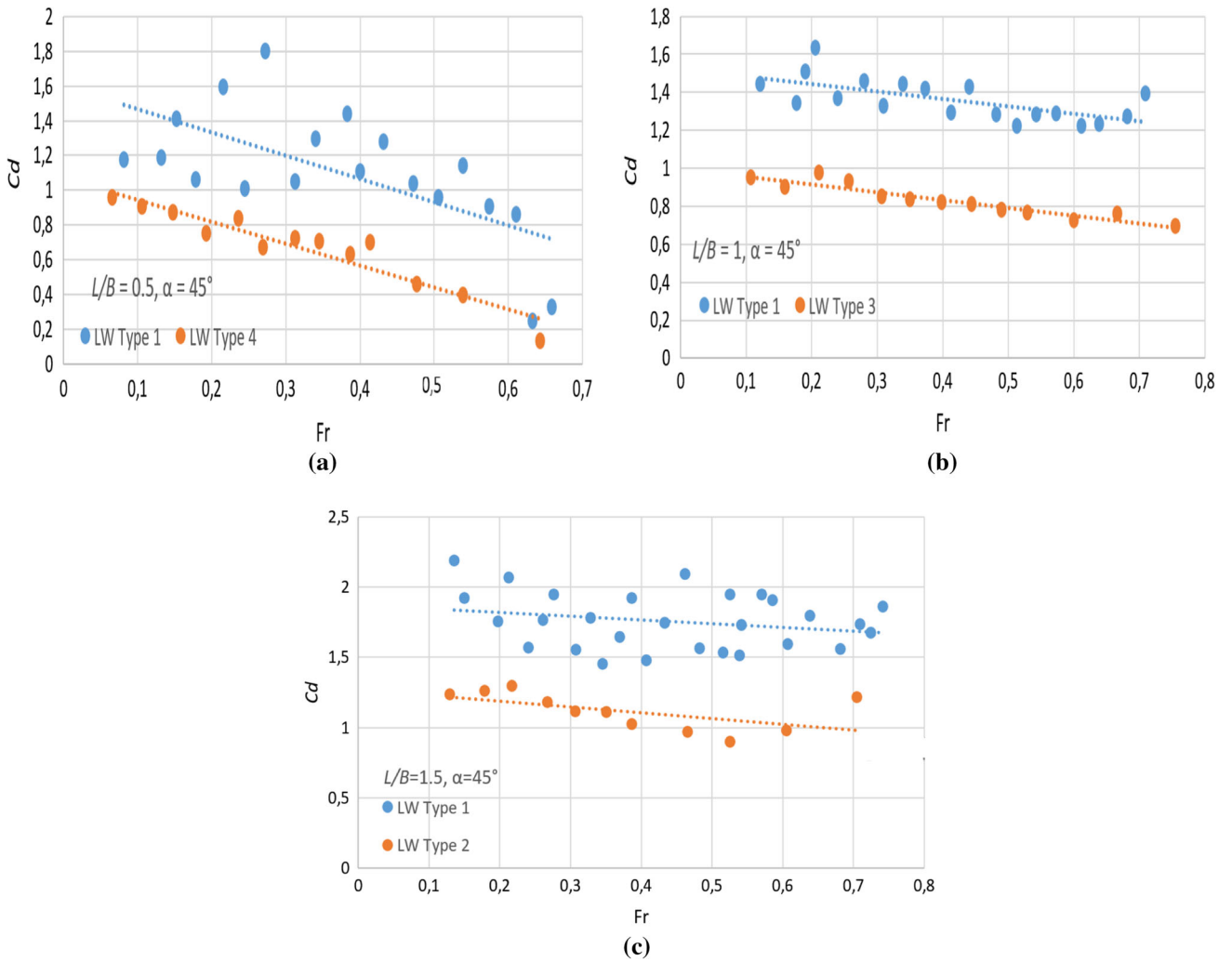|	L	P	θ	Crest contraction ratio	Decrease in discharge capacity (%)	Mean decrease in discharge capacity (%)
1	25	12	45	1/3	8	
2	25	16	45	1/3	10	
3	25	20	45	1/3	30	
4	50	12	45	1/3	23	
5	50	16	45	1/3	28.5	
6	50	20	45	1/3	29.5	
7	75	12	45	1/3	31.5	
8	75	16	45	1/3	34	
9	75	20	45	1/3	38	
10	25	12	90	1/3	11	
11	25	16	90	1/3	11	
12	25	20	90	1/3	8	
13	50	12	90	1/3	11	19
14	50	16	90	1/3	8	
15	50	20	90	1/3	21.5	
16	75	12	90	1/3	38.5	
17	75	16	90	1/3	24	
18	75	20	90	1/3	21.5	
19	25	12	150	1/3	4	
20	25	16	150	1/3	16.5	
21	25	20	150	1/3	23.5	
22	50	12	150	1/3	5	
23	50	16	150	1/3	23	
24	50	20	150	1/3	7	
25	75	12	150	1/3	13.5	
26	75	16	150	1/3	12.5	
27	75	20	150	1/3	11.5	
28	25	12	45	2/3	23	
29	25	16	45	2/3	41	
30	25	20	45	2/3	47	
31	50	12	45	2/3	37.5	
32	50	16	45	2/3	36.5	
33	50	20	45	2/3	37.5	
34	75	12	45	2/3	37.5	
35	75	16	45	2/3	44	
36	75	20	45	2/3	46	
37	25	12	90	2/3	37.5	
38	25	16	90	2/3	15	
39	25	20	90	2/3	16.5	32
40	50	12	90	2/3	24	
41	50	16	90	2/3	28.5	
42	50	20	90	2/3	27.5	
43	75	12	90	2/3	37.5	

Table 2 (continued)

	L	P	θ	Crest contraction ratio	Decrease in discharge capacity (%)	Mean decrease in discharge capacity (%)
44	75	16	90	2/3	39	
45	75	20	90	2/3	26	
46	25	12	150	2/3	17	
47	25	16	150	2/3	40	
48	25	20	150	2/3	21.5	
49	50	12	150	2/3	21.5	
50	50	16	150	2/3	32	
51	50	20	150	2/3	23	
52	75	12	150	2/3	30.5	
53	75	16	150	2/3	30	
54	75	20	150	2/3	23.5	
55	25	12	45	3/3	23.5	
56	25	16	45	3/3	40	
57	25	20	45	3/3	44	
58	50	12	45	3/3	44.5	
59	50	16	45	3/3	47	
60	50	20	45	3/3	50	
61	75	12	45	3/3	45.5	
62	75	16	45	3/3	51	
63	75	20	45	3/3	56	
64	25	12	90	3/3	45	
65	25	16	90	3/3	20.5	
66	25	20	90	3/3	34	
67	50	12	90	3/3	40	
68	50	16	90	3/3	38.5	
69	50	20	90	3/3	44.5	42
70	75	12	90	3/3	45	
71	75	16	90	3/3	43	
72	75	20	90	3/3	43	
73	25	12	150	3/3	36.5	
74	25	16	150	3/3	35.5	
75	25	20	150	3/3	46	
76	50	12	150	3/3	34.5	
77	50	16	150	3/3	45	
78	50	20	150	3/3	36	
79	75	12	150	3/3	42.5	
80	75	16	150	3/3	42.5	
81	75	20	150	3/3	43.5	

3.1 Variation of Discharge Coefficient at Triangular Labyrinth Side Weir

To implement the De Marchi method, which is one of the most common and basic principles in the design of side weirs, the main channel must be arranged as a rectangular sectional. Otherwise, the method should be adapted for the cross-sectional area. Adoption of constant specific energy must be ensured for upstream and downstream of the side weir. Since the tests were carried out in an open channel with a rectangular section, the De Marchi equation was applied without the need for any adaptation. Moreover, the negligible condition of the difference in the specific energy between the side weir upstream and the downstream must be taken into
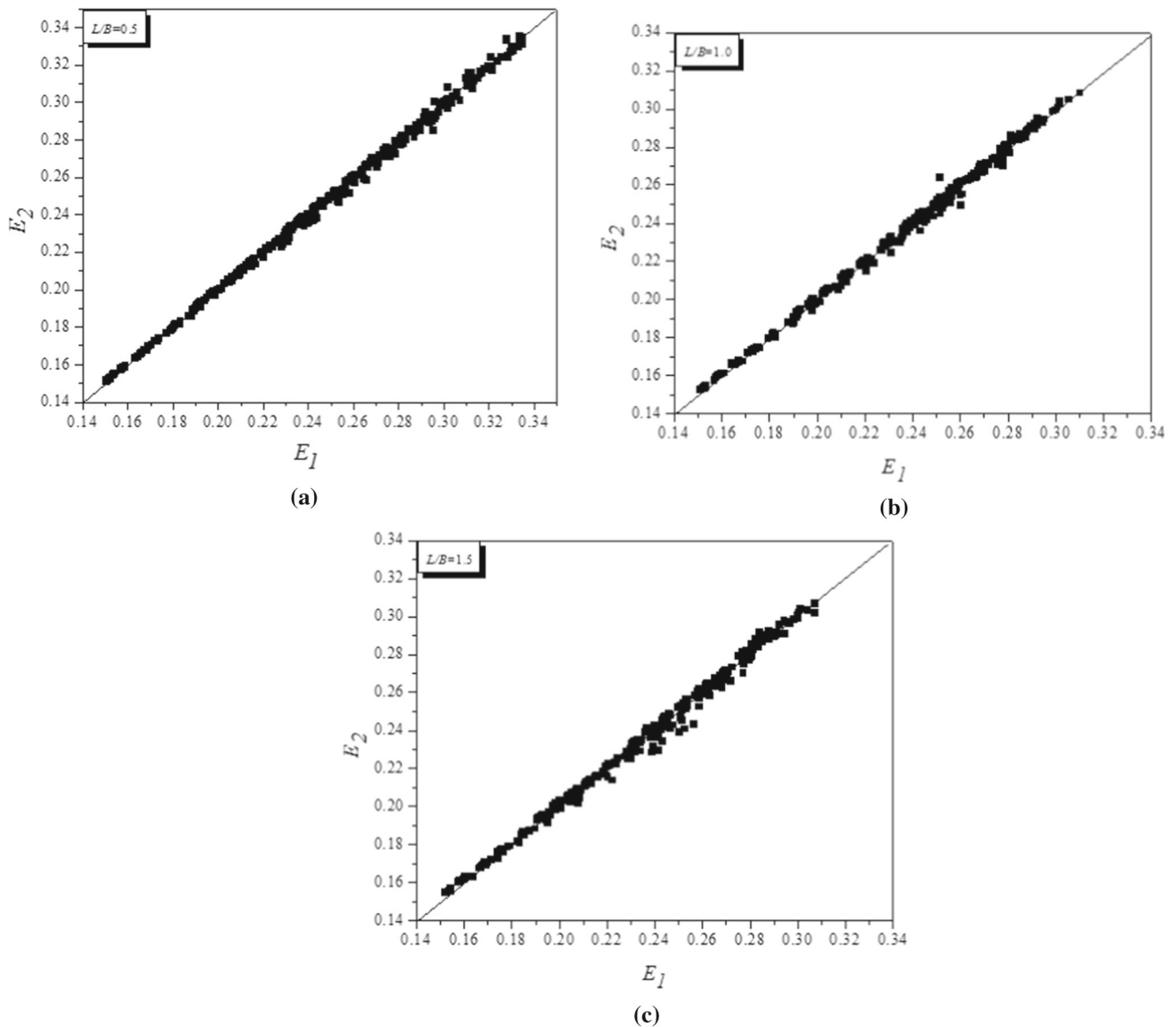
Fig. 5 **a–c** Comparison of E_1 and E_2 in the straight channel

account for the use of the De Marchi equation (< % 4). As can be seen in Fig. 5, almost all values were seen to have converged to the 45° line in the graphs of E_1 and E_2 values drawn for different *L/B* ratios. Since the average difference between E_1 and E_2 was found to be approximately 0.09% as a result of the calculations, it was concluded that the De Marchi approach could be safely applied.

3.1.1 Effect of Non-dimensional Nappe Height

The *$(y_1 - p)$/p* values versus C_d are given in the graphs in Figs. 6, 7, 8 to reveal the effect of the *$(y_1 - p)$/p* parameter on the discharge coefficient. Figures 6, 7, 8 show that as the *$(y_1 - p)$/p* value increases, the discharge coefficient decreases. Khode et al. [13] found that the discharge capacity in filled

labyrinth weirs decreased as the nappe load increased. Similarly, in this study, a decrease in discharge capacity was observed as the nappe load increased. When the flow depth is low, the flow freely falls along the entire length of the weir. The airflow could be accessed from the downstream and the corners. Emiroglu et al. [11] showed that this decreasing tendency was higher at low slope angles. In Figs. 6, 7, 8, the flow on the top varies with the increase in nappe, because of the flow over the side weirs.

Figure 6 shows the variation between C_d and *$(y_1 - p)$/p* for the triangular labyrinth side weir with $\alpha = 45°$ apical angle in the linear channel. As seen in Fig. 6a, it is observed that the *$(y_1 - p)$/p* value coincided at around 0.22 for fully open and 1/3 open statuses at the *L/B* = 0.5 ratio. The discharge coefficient values determined in the fully open state are higher than the
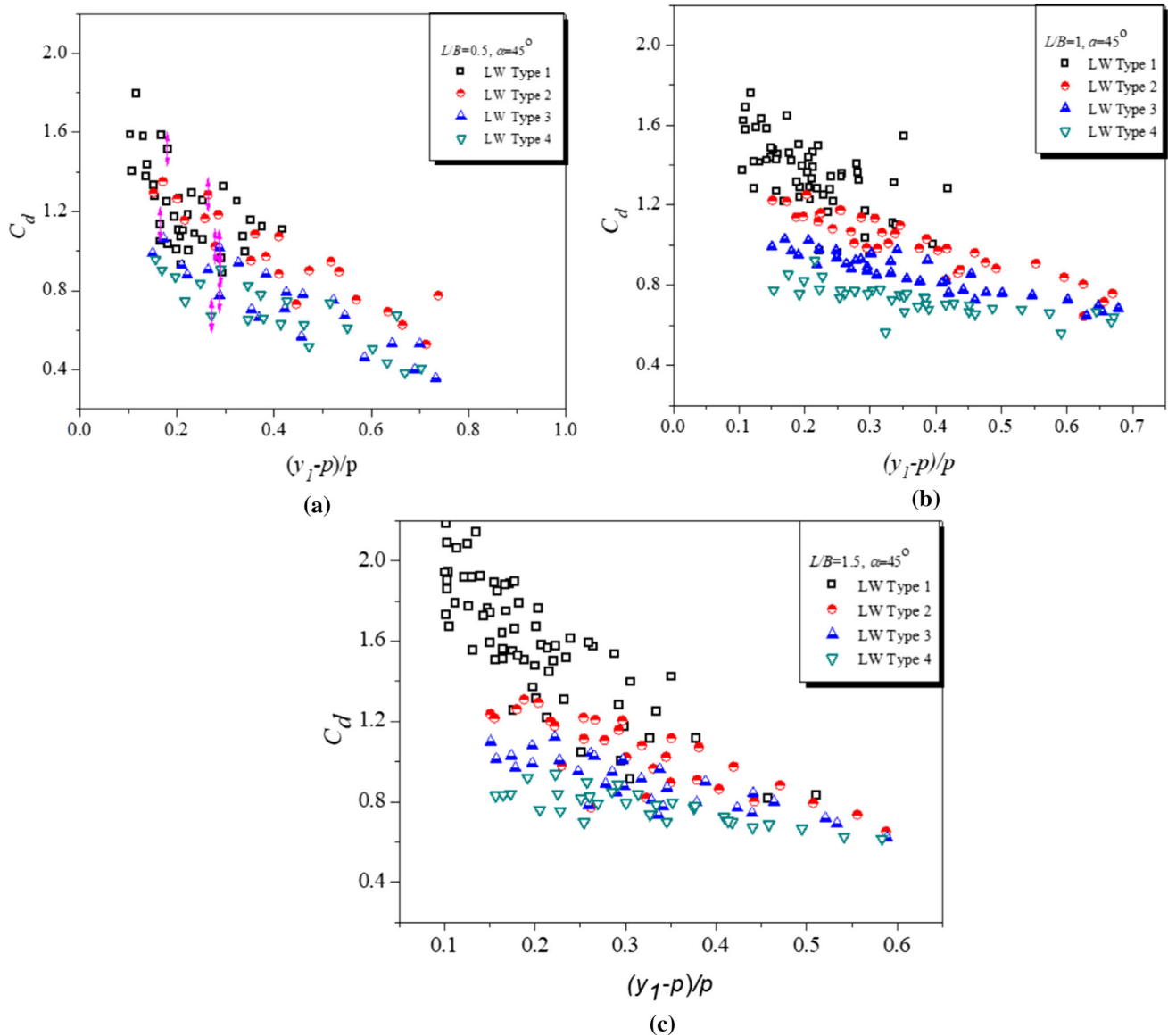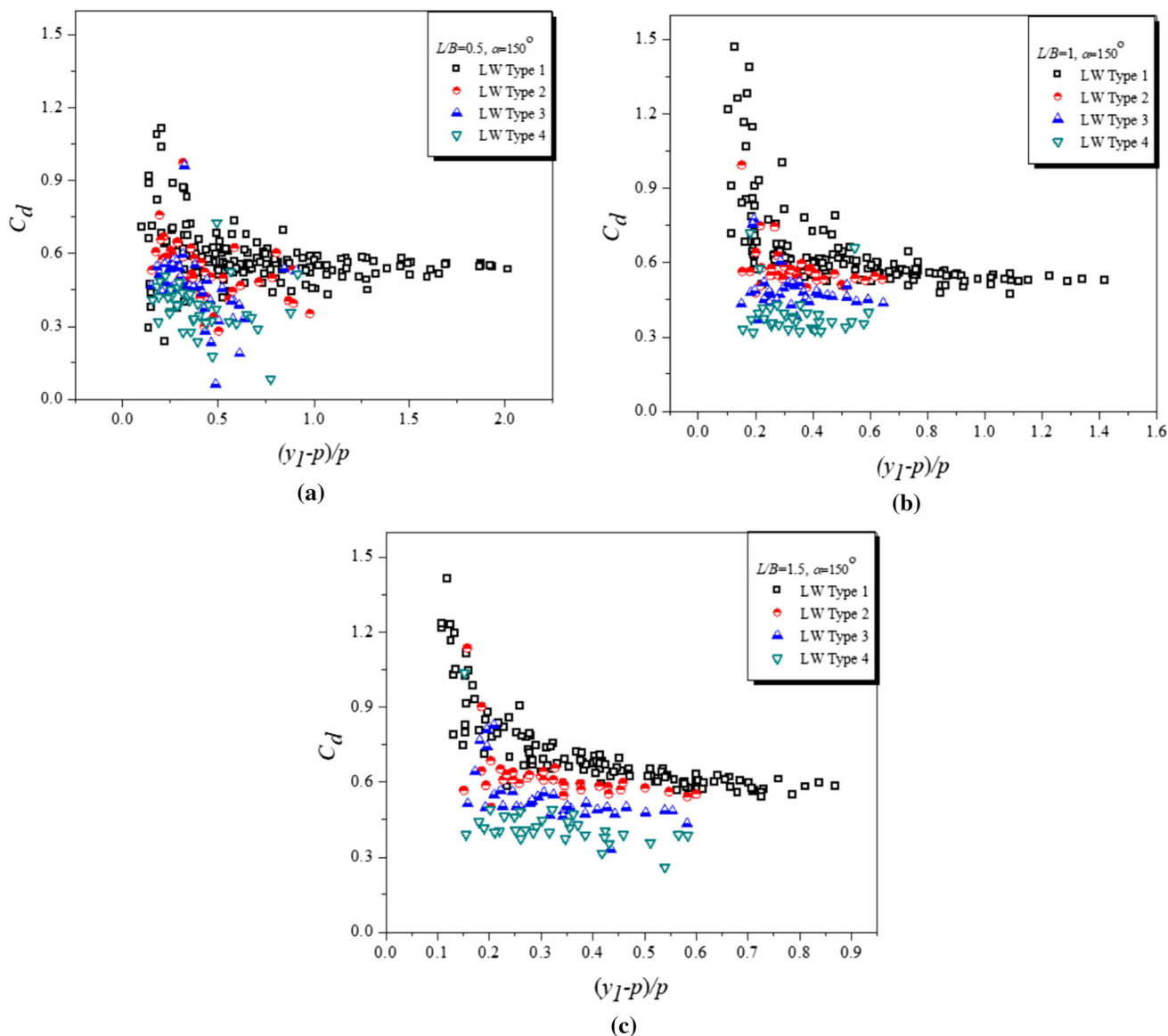
Fig. 6 Variation of discharge coefficient (C_d) against the $(y_1 - p)/p$ for different upstream constrictions at $\alpha = 45°$ in the straight channel: **a** L/B = 0.5 **b** L/B = 1.0 **c** L/B = 1.5

1/3 closed state for the 0.1 to 0.22 interval of $(y_1 - p)/p$. All three graphs in Fig. 6 show that the value of the discharge coefficient is at the maximum in the fully open state. The value of the discharge coeffient decreases successively in the 1/3, 2/3 and 3/3 closed states. In addition, in Fig. 6c, the slope of the curve fitted to the discharge coefficient values for the fully open state is more perpendicular than the other curves representing the other cases. In other words, a decrease was seen in the discharge coefficient at higher rates. The fact that the L/B was at the maximum value in the tests where these data were obtained was considered to be the reason for this.

Figure 7 shows the variation between C_d and $(y_1 - p)/p$ for the triangular labyrinth side weir with $\alpha = 90°$ included angle in the linear channel. In Fig. 7 (a), the variation in

the fully open status is seen to be smaller. This is different in other cases. When Fig. 7a–c is examined, it is seen that there is an inverse correlation between the $(y_1 - p)/p$ and C_d values. The maximum values of the discharge coefficient are seen in the fully open state. This is followed by 1/3, 2/3, and 3/3 closed states, respectively. As shown in Figs. 7a–c, as the L/B ratio increases, an increase is seen in the discharge coefficient for the fully open state. In addition, Fig. 7a shows that the curves are close to each other when the $(y_1 - p)/p$ values are minimum. However, this is not seen in Fig. 7b and c.

Figure 8 shows the variation between C_d and $(y_1 - p)/p$ for the triangular labyrinth side weir with $\alpha = 150°$ included
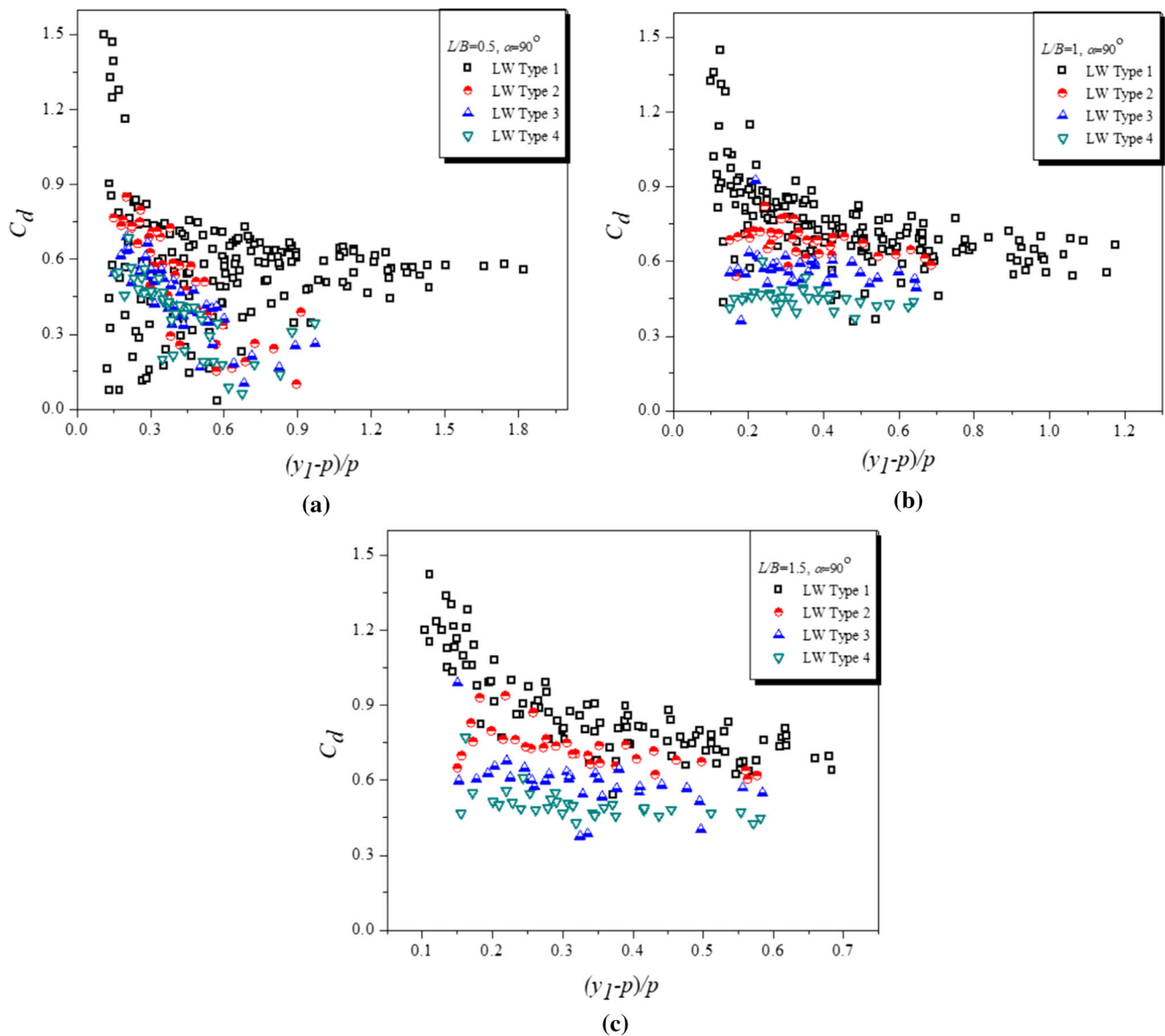
Fig. 7 Variation of discharge coefficient (C_d) against the $(y_1 − p)/p$ for different upstream constrictions at $\alpha = 90°$ in the straight channel: **a** *L/B* = 0.5 **b** *L/B* = 1.0 **c** *L/B* = 1.5

angle in the linear channel. The sorting of the discharge coefficient in Fig. 8a–c from the minimum to the maximum is 3/3 closed, 2/3 closed, 1/3 closed and fully open states, respectively. It is understood from this that the discharge coefficient decreases with the reduction of the total crest length.

3.1.2 Effect of the Froude Number

Figures 9, 10, 11 show the variation of the discharge coefficient of the Froude number together with the fully open, 1/3, 2/3, and 3/3 different non-dimensional weir crest lengths for the *L/B* = 0.50, 1.0, 1.5 non-dimensional weir widths. It is seen that the discharge coefficient (C_d) decreases with increasing Froude number (Fr). In Fig. 9a, the fully open and

1/3 closed states appear to have values close to each other in low Froude numbers. However, it is seen that 2/3 and 3/3 closed states receive values close to each other with an increasing Froude number and a decreasing discharge coefficient. The result from the graphs in Fig. 9a–c proves that the best discharge coefficient for the *L/B* = 0.5, 1.0, 1.5 ratios are obtained when it is fully open. With the decreases of effective crest lengths at 1/3, 2/3, and 3/3 rates for *L/B* = 0.50, respectively, decreases in discharge capacity are observed. When closure rates and completely open situations are considered, the decrease rates of 1/3, 2/3, and 3/3 closure situations, compared to completely open situations, are observed as 16%, 26% and 37%, respectively. As a result of the closure of the effective crest length, the decreases in discharge capacity are
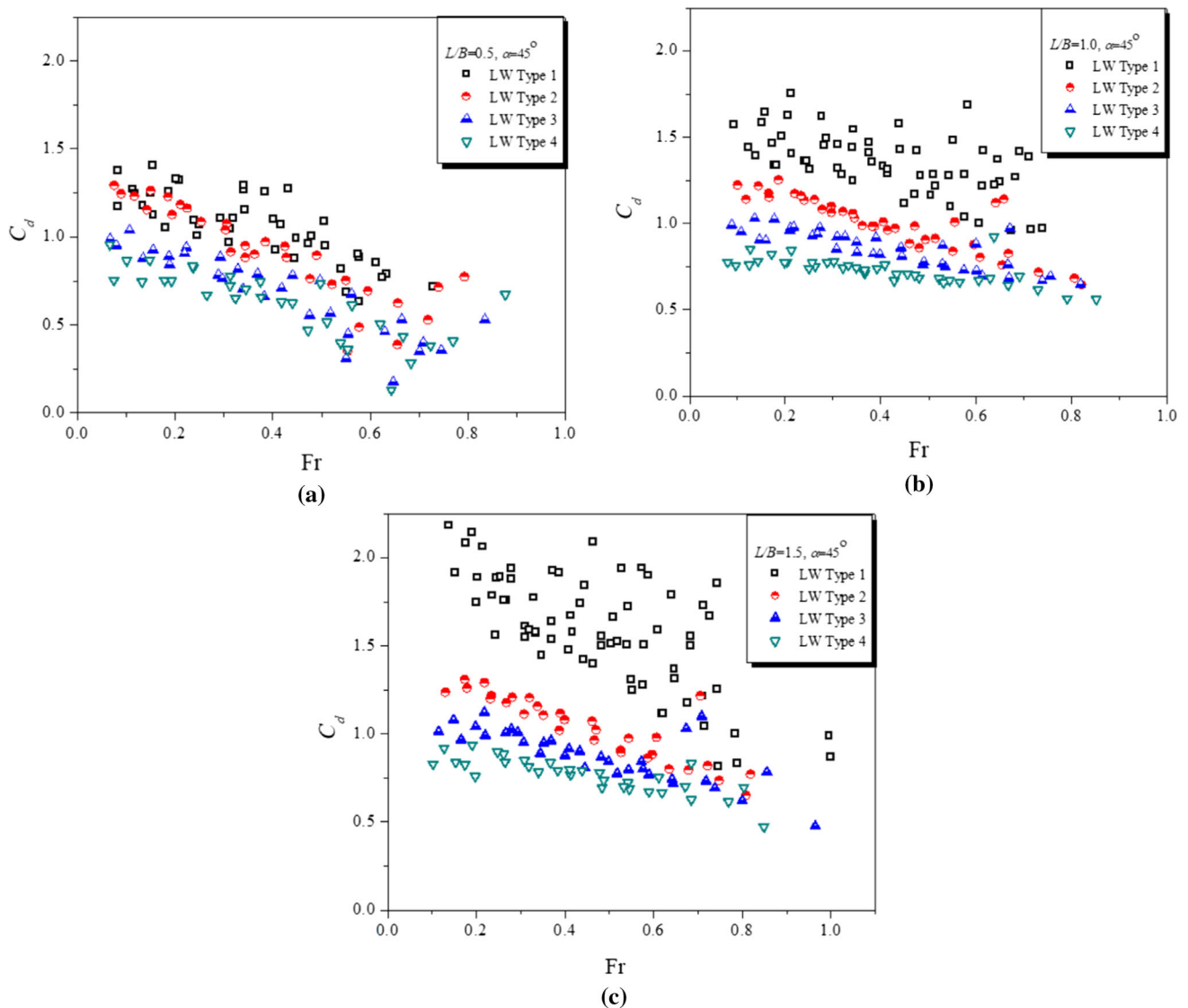
Fig. 8 Variation of discharge coefficient (C_d) against the $(y_1 - p)/p$ for different upstream constrictions at $\alpha = 150°$ in the straight channel: **a** *L/B* = 0.5 **b** *L/B* = 1.0 **c** *L/B* = 1.5

also present for $L/B = 1.0$ and 1.5. However, the changes are not at significant rates. These rates are observed as 27%, 37.5%, 47% and 34%, 42.5%, 51%. As shown in Fig. 9, it is seen that the (C_d) is more variable (diffuse) in the fully open state.

Figure 10 shows the relationship between the Froude number and the discharge coefficient at different L/B ratios for $\alpha = 90°$ in the linear channel. Figure 10a–c shows a decrease in the discharge coefficient when the Froude number increases. The state when the discharge coefficient is the at maximum value is when it is fully open and the state when it is at the minimum value is when it is 3/3 closed. The discharge coefficient values in Fig. 10c vary more compared to the other graphs.

In Fig. 10a, it is seen that the values for the 1/3 closed state converge to the values of the fully open state in low values of Froude numbers and the values of the 2/3 closed state in high values of Froude numbers. With the decreases of effective crest lengths at 1/3, 2/3, and 3/3 rates for $L/B = 0.50$, respectively, decreases in discharge capacity are observed. When closure rates and completely open situations are considered, the decrease rates of 1/3, 2/3, and 3/3 closure situations, compared to completely open situations, are observed as 10%, 23% and 33%, respectively. As a result of the closure of the effective crest length, the decreases in discharge capacity are also present for L/B = 1.0 and 1.5. However, the changes
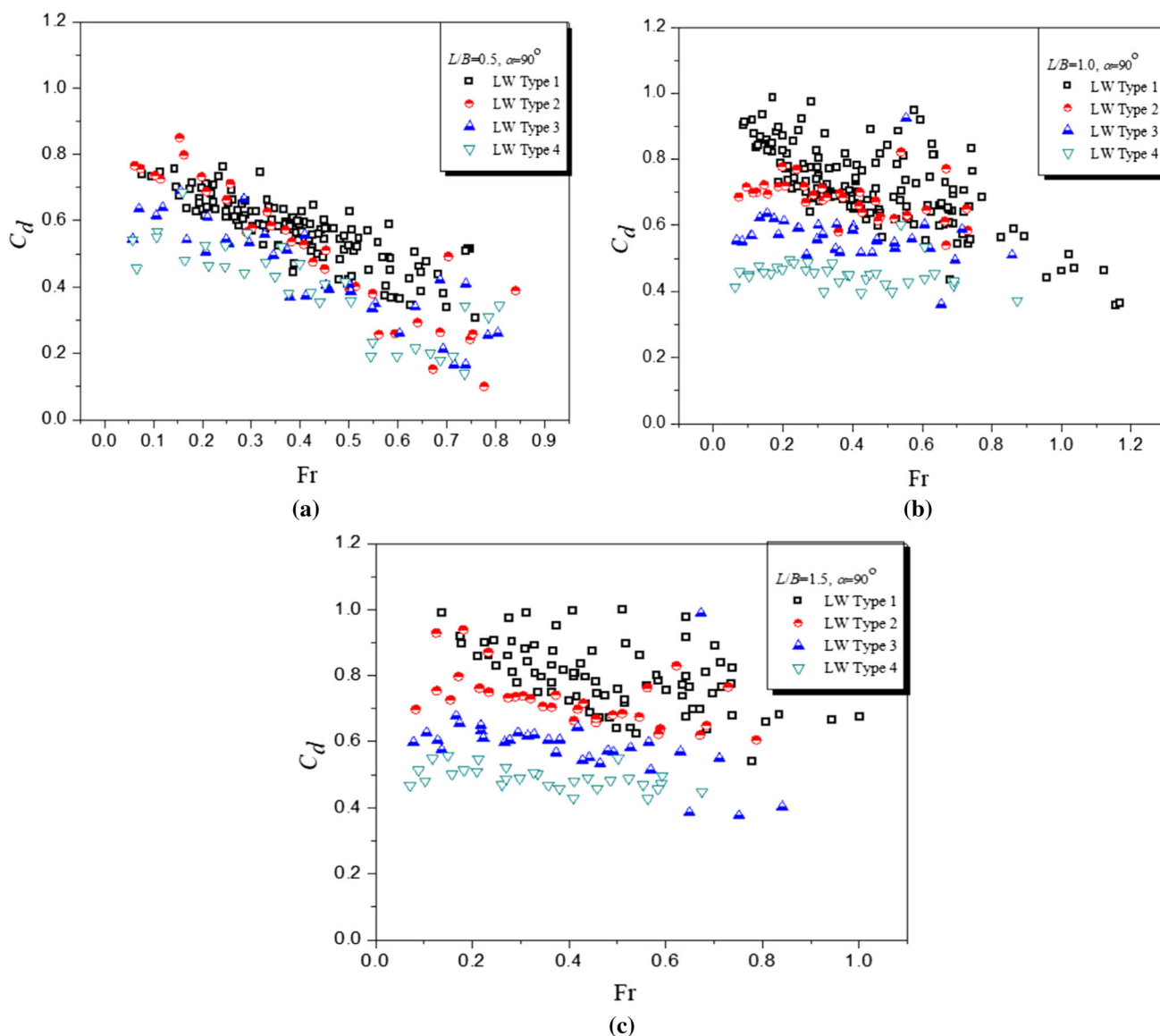
Fig. 9 Variation of discharge coefficient (C_d) against the Froude number (Fr) for different upstream constrictions at $\alpha = 45°$ in the straight channel: **a** $L/B = 0.5$ **b** $L/B = 1.0$ **c** $L/B = 1.5$

are not at significant ratios. These rates are observed as 14%, 27%, 41% and 28%, 34%, 44%, respectively.

Figure 11 shows the relationship between the Froude number and the discharge coefficient at different L/B ratios for $\alpha = 150°$ in the linear channel. Figure 11 shows that the discharge coefficient decreases with the increasing Froude number. It is seen that the order of the discharge coefficient has not changed. With the decreases of effective crest lengths at 1/3, 2/3, and 3/3 rates for $L/B = 0.50$, respectively, decreases in discharge capacity are observed. When closure rates and completely open situations are considered, the decrease rates of 1/3, 2/3, and 3/3 closure situations, compared to completely open situations, are observed as 15%, 26% and 40%, respectively. As a result of the closure of the effective crest length, the decreases in discharge capacity are also present for $L/B = 1.0$ and 1.5. However, the changes are not at significant ratios. These rates are observed as 12%, 25.5%, 39% and 12.5%, 28%, 43%, respectively.

Fig. 10 Variation of discharge coefficient (C_d) against the Froude number (Fr) for different upstream constrictions at $\alpha = 90°$ in the straight channel: **a** $L/B = 0.5$ **b** $L/B = 1.0$ **c** $L/B = 1.5$

4 Conclusions

Based on the results of this experimental study on the labyrinth side weir crest narrowing, the findings obtained are presented below.

- It was observed that as the values of the Froude number were increased; the discharge coefficient decreased, which was in line with the literature. Similarly, as the L/B ratio increased, increases in discharge coefficient were observed.
- For different flow conditions, the maximum discharge coefficient in the completely open situation was observed in the triangle labyrinth side weir.

- In the experiments conducted by closing the upstream crest lengths at 1/3, 2/3, and 3/3 ratios for flow, the obtained discharge coefficient values were the highest.
- When the labyrinth side weir upstream crest length was closed at a 1/3 ratio, the mean decrease was 19%. When it was at a 2/3 ratio, this value was 32% while it was 42% at a 3/3 ratio. To calculate the overflow discharge due to the decreases in the crest, these percentage values can be utilized reliably. For double-end closure ratios, it is possible to use these values and conduct interpolation. In conclusion, based on the experiments conducted on linear canals, decreases in the triangular labyrinth side weir upstream crest lengths cause decreases in discharge coefficient.
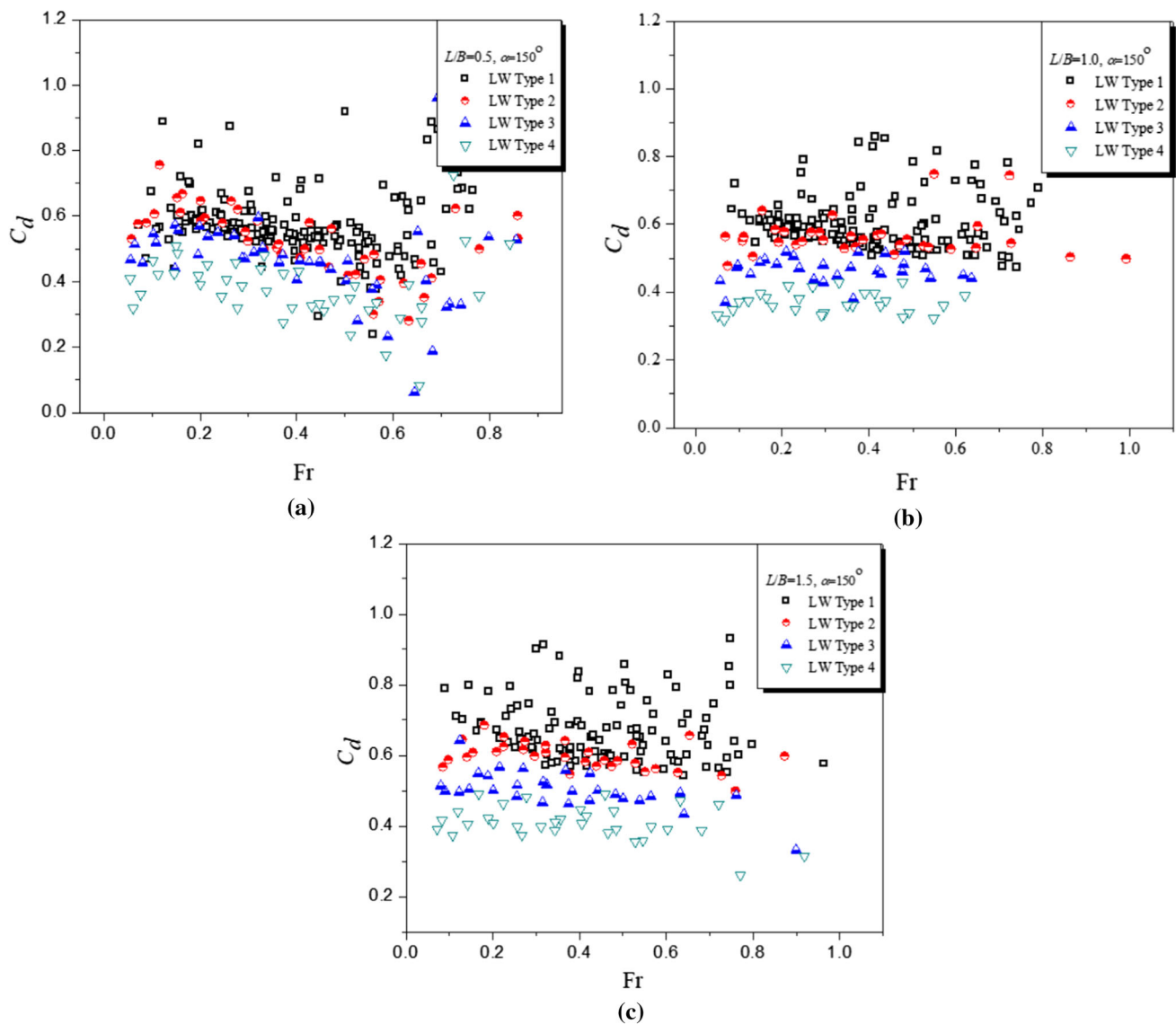
Fig. 11 Variation of discharge coefficient (C_d) against the Froude number (Fr) for different upstream constrictions at $\alpha = 150°$ in the straight channel: **a** $L/B = 0.5$ **b** $L/B = 1.0$ **c** $L/B = 1.5$

- If the stream floor is a movable base; Swab materials from the main channel may accumulate in front of the weir crest, reducing the weir crest size. In this case, there will be no spillet along the entire crest. Similarly, a certain portion of the weir crest may be covered by debris. In this case, the effective weir length is reduced. In this study, how much the discharge capacity would decrease in such a case was determined by experimental study and it was predicted that studies on the reduction of discharge capacity could be done by using different weir types in future studies.

References

1. Ansari, U.; Patil, L.: Numerical analysis of triangular labyrinth side weir in triangular channel. ISH J. Hydraul. Eng. **28**(sup1), 141–148 (2022)
2. Ikinciogulları, E.; Emiroglu, M.: Estimation of triangular labyrinth side weir discharge capacity using schmidt approach. Sigma J. Eng. Nat. Sci. **37**(1), 289–303 (2019)
3. Kilic, Z.; Emin Emiroglu, M.: Study of hydraulic characteristics of trapezoidal piano key side weir using different approaches. Water Supply **22**(8), 6672–6691 (2022)
4. Ben Said, M.; Ouamane, A.: Performance of rectangular labyrinth weir–an experimental and numerical study. Water Supply **22**(4), 3628–3644 (2022)

5. Emiroglu, M.E.; Gogus, M.; Tunc, M.; Islamoglu, K.: Effects of antivortex structures installed on trapezoidal labyrinth side weirs on discharge capacity and scouring. J. Irrig. Drain. Eng. **143**(6), 04017006 (2017)

6. Cosar, A.; Agaccioglu, H.: Discharge coefficient of a triangular side-weir located on a curved channel. J. Irrig. Drain. Eng. **130**(5), 410–423 (2004)

7. Aydin, M.; Emiroglu, M.: Determination of capacity of labyrinth side weir by CFD. Flow Meas. Instrum. **29**, 1–8 (2013)

8. Emiroglu, M.E.; Kaya, N.; Agaccioglu, H.: Discharge capacity of labyrinth side weir located on a straight channel. J. Irrig. Drain. Eng. **136**(1), 37–46 (2010)

9. Emiroglu, M.E.; Aydin, M.C.; Kaya, N.: Discharge characteristics of a trapezoidal labyrinth side weir with one and two cycles in subcritical flow. J. Irrig. Drain. Eng. (2014). https://doi.org/10.1061/(ASCE)IR.1943-4774.0000709

10. De Marchi, G.: Essay on the performance of lateral weirs. L'Energia Electtrica Milano. **11**(11), 849–860 (1934)

11. Emiroglu, M.E.; Agaccioglu, H.; Kaya, N.: Discharging capacity of rectangular side weirs in straight open channels. Flow Meas. Instrum. **22**(4), 319–330 (2011)

12. Novák, P.; Cabelka, J.: Models in Hydraulic Engineering; Physical Principles and Design Applications. Pitman Advanced Publishing Program (1981)

13. Khode, B.V.; Tembhurkar, A.R.; Porey, P.D.; Ingle, R.N.: Experimental studies on flow over Labyrinth Weir. J. Irrig. Drain. Eng. **10**, 1061 (2012)